

Microlensing variability in time-delay quasars

Danuta Paraficz^{1,2}, Jens Hjorth¹, Ingunn Burud³, Páll Jakobsson¹, and Árdís Elíasdóttir¹

¹ Dark Cosmology Centre, Niels Bohr Institute, University of Copenhagen, Juliane Maries Vej 30, DK-2100 Copenhagen, Denmark e-mail: danutas@astro.ku.dk

² Nordic Optical Telescope (NOT), Apartado 474, 38700 Santa Cruz de La Palma, Canary Islands, Spain

³ Norwegian Meteorological Institute, P.O. Box 43, Blindern, N-031 3 Oslo, Norway

Received March 26, 2006

ABSTRACT

We have searched for microlensing variability in the light curves of five gravitationally lensed quasars with well-determined time delays: SBS 1520+530, FBQ 0951+2635, RX J0911+0551, B1600+434 and HE 2149–2745. By comparing the light curve of the leading image with a suitably time offset light curve of a trailing image we find that two (SBS 1520+530 and FBQ 0951+2635) out of the five quasars have significant long-term (\sim years) and short-term (\sim 100 days) brightness variations that may be attributed to microlensing. The short-term variations may be due to nanolenses 10^{-4} – $10^{-3} M_{\odot}$, relativistic hot or cold spots in the quasar accretion disks, or coherent microlensing at large optical depth.

Key words. gravitational lensing – quasars: individual: SBS 1520+530, FBQ 0951+2635, RX J0911+0551, B1600+434, HE 2149-2745

1. Introduction

The effect of a background source being gravitationally lensed by foreground compact objects is known as microlensing. Chang & Refsdal (1979) predicted that in lensed quasar systems the light path should be affected by stars in the lensing galaxy. Moving compact objects in the lensing galaxy can cause spectral changes, brightness variability and, in the case of multiple images, flux ratio anomalies in the lensed quasar. When the foreground galaxy causes multiple images of the quasar, photometric monitoring can be used to isolate intrinsic quasar variability from microlensing variability by comparison of the separate light curves. Likewise, spectral differences between quasar images, caused by differential magnification across the quasar, can be directly detected in multiply imaged quasars. Microlensing offers the opportunity to study the nature of matter in foreground galaxies and the spatial structure of the lensed quasar at very high angular resolution (Kochanek 2004). The first quasar microlensing events were discovered 17 years ago by Irwin et al. (1989) and Schild (1990).

In this Letter we analyze the light curves of five lensed quasars for which a time delay has previously been measured in dedicated monitoring campaigns (Burud et al. 2000, 2002a,b; Hjorth et al. 2002; Jakobsson et al. 2005). Four of them were observed at the Nordic Optical Telescope (NOT) between 1998–2002 and one (HE 2149–2745) was observed at the Danish 1.5-m telescope. We here examine the light curves for microlensing variability and at the same time make all data points available online.

Send offprint requests to: D. Paraficz

Table 1. Properties of the lens systems. The time delays were obtained by: 1. Burud et al. (2002b), 2. Jakobsson et al. (2005), 3. Burud et al. (2002a), 4. Hjorth et al. (2002), 5. Burud et al. (2000).

Name	z_l	z_s	Δt (days)	Separation	Ref.
SBS 1520+530	0.72	1.86	130 ± 2	$1.57''$	1
FBQ 0951+2635	0.24	1.25	16 ± 2	$1.10''$	2
HE 2149–2745	0.495	2.03	103 ± 12	$1.70''$	3
RX J0911+0551	0.77	2.80	146 ± 4	$3.10''$	4
B1600+434	0.41	1.59	51 ± 2	$1.38''$	5

2. Analysis

The images of a lensed quasar may vary due to intrinsic quasar brightness changes and/or microlensing. Microlensing affects the light paths of each image differently (in the simplest case only one path is affected) whereas the intrinsic variations show up in all the images but at different times due to the time delay. Therefore, one can isolate the microlensing signal by calculating the difference between two light curves, suitably shifted in time to correct for the time delay.

Observationally, quasar light curves suffer from sampling effects leading to a need for interpolation. Due to their small separations and the presence of the lensing galaxy they may also potentially be affected by systematic errors in the photometry. To eliminate artifacts arising from such effects we do not interpolate data points with a gap bigger than a time delay of a system and we require that the light curve difference be (1) uncorrelated with the quasar variations and (2) independent of

which image light curve we interpolate. These are conservative criteria for detection of a microlensing signal in the light curves which ensure that the signal is reliable and robust. If the criteria are violated the variability may be the result of observational, systematic or interpolation errors.

3. Results

Were we apply the analysis to the five quasar light curves to search for microlensing events.

3.1. SBS 1520+530

The doubly imaged quasar SBS 1520+530 (see Table 1) was monitored between February 1999 and May 2001 at the NOT. In Fig. 1 we show the light curves of the two images, A and B, where B has been shifted in both time (-130 days) and brightness (-0.69 mag). Also shown are the magnitude residuals, Δm , obtained by linear interpolation of one of the images. The middle panel shows the difference between a linearly interpolated A light curve and the B data points (Δm_{AB}). The lower panel shows the difference between a linearly interpolated B light curve and the A data points (Δm_{BA}). Any deviation from a constant difference lightcurve (dashed horizontal line) can be attributed to microlensing. In both residual plots one notices a constant magnitude increase and an approximately 200-day-wide magnitude bump. In the following we characterize such residuals phenomenologically using linear or Gaussian fits.

A linear fit shows that the slopes of the plots are 0.0073 ± 0.0014 mag/100 days for Δm_{AB} and 0.0070 ± 0.0016 mag/100 days for Δm_{BA} . The agreement between these values indicates that the mean difference between the images increases by about 0.007 mag per 100 days. This is consistent with the observations of Gaynullina et al. (2005) who found an increase in the magnitude difference between the quasar images of 0.14 ± 0.03 mag over 1500 days (0.009 ± 0.002 mag/100 days). We interpret this signal as evidence for microlensing.

A Gauss function with baseline zero, fitted to the bump for Δm_{AB} gives a FWHM of 220 ± 42 days and a peak magnitude variation of 0.053 ± 0.008 mag. For Δm_{BA} the FWHM is 183 ± 29 days and the peak magnitude variation is 0.063 ± 0.009 mag. These values are consistent within the errors.

Microlensing in SBS 1520+530 was already detected spectroscopically by Burud et al. (2002b) who analyzed continuum normalized spectra and showed that the equivalent widths of emission lines in A were larger than in B.

3.2. FBQ 0951+2635

The doubly imaged quasar FBQ 0951+2635 (see Table 1) was observed between March 1999 and June 2001 at the NOT. Spectroscopic indications of possible microlensing in the system were found by Schechter et al. (1998) and Jakobsson et al. (2005).

We repeat the microlensing-extraction procedure described above for FBQ 0951+2635. In Fig. 2 we show the light curves of the two images, A and B, the latter shifted in time by -16 days and in brightness by -1.06 mag. The middle and lower

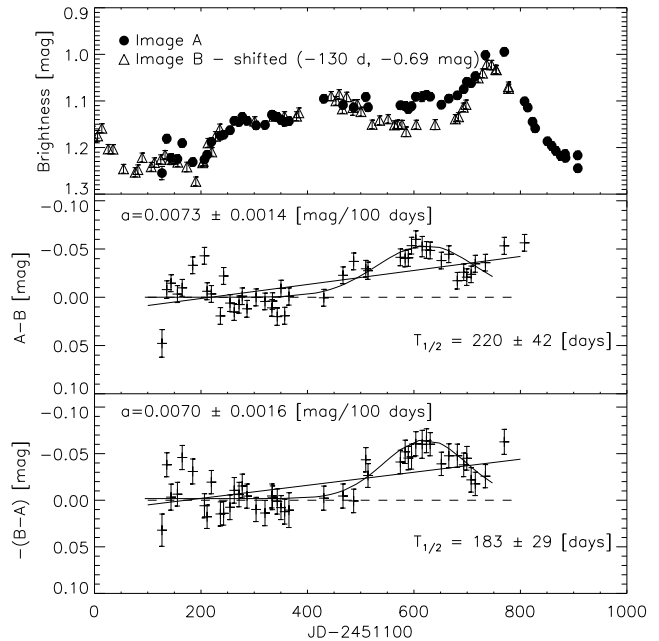


Fig. 1. R-band light curves of SBS 1520+530. **Top:** Time-delay shifted light curves, with the B image offset by -0.69 mag and -130 days. **Middle:** Difference between linearly interpolated A image and B image. **Bottom:** Difference between linearly interpolated B image and A image. The middle and bottom panels also present linear fits (where a is the slope) and Gaussian fits (where $T_{1/2}$ is the FWHM) to the data.

panels show Δm_{AB} and Δm_{BA} . In both plots one notices a constant magnitude increase and a bump at the beginning of the observations.

Linear fits to the data yield slopes of 0.0095 ± 0.0011 and 0.0077 ± 0.0007 mag/100 days for Δm_{AB} and Δm_{BA} respectively. A Gauss function with baseline zero, fitted to the bump for Δm_{AB} gives a FWHM of 151 ± 111 days and a peak magnitude variation of 0.048 ± 0.009 mag. For Δm_{BA} gives FWHM of 81 ± 27 days and a peak magnitude variation of 0.061 ± 0.016 mag. These values are consistent within the errors.

3.3. Quasars where no microlensing is confirmed

The three quasars where no microlensing variability was reliably detected are the double quasar HE 2149–2745 observed at the Danish 1.5-m telescope, ESO-La Silla (October 1998 – December 2000), the quadruple quasar RX J0911+0551 observed at the NOT (March 1997 – April 2001), and the doubly imaged quasar B1600+434 observed at the NOT (April 1998 – November 1999) (see Table 1).

Plots similar to Figs. 1 and 2 are shown in Figs. 3–5. For HE 2149–2745 (Fig. 3) and RX J0911+0551 (Fig. 4) we see some long term variations in the light curve difference but the analysis shows that the slopes differ depending on which of the two light curves are interpolated. In B1600+434 (Fig. 5) one sees clear magnitude variations in the light curve differences but they do not satisfy our second condition for microlensing.

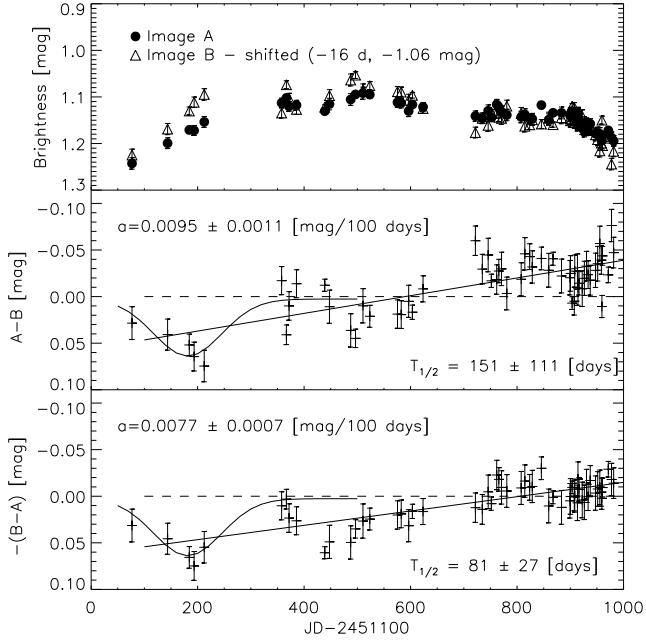


Fig. 2. R-band light curves of FBQ 0951+2635. **Top:** Time-delay shifted light curves, with the B image offset by -1.06 mag and -16 days. **Middle:** Difference between linearly interpolated A image and B image. **Bottom:** Difference between linearly interpolated B image and A image. The middle and bottom panels also present linear fits (where a is the slope) and Gaussian fits (where $T_{1/2}$ is the FWHM) to the data.

By comparison with the top plot we see that they are correlated with the quasar variations (the magnitude bump appears at ~ 420 days on all plots).

Thus, while we detect intriguing light curve differences and cannot rule out microlensing variability in these systems, this indicates that the detected magnitude changes may also be attributed to photometric or interpolation errors.

4. Discussion

We have demonstrated the existence of a short-term microlensing variability in the photometric data sets of the two quasar systems SBS 1520+530 and FBQ 0951+2635. Interestingly, microlensing has previously been detected spectroscopically and as flux anomalies in both systems (Burud et al. 2002b; Faure et al. 2002; Schechter et al. 1998; Jakobsson et al. 2005). We note that the time scales of the short-term variability detected in the quasars (50–200 days) is similar to the ‘90 day’ events in QSO Q0957+561A,B (see Schild 1996).

In principle one can calculate the masses of the lenses responsible for the microlensing from the time scales of brightness variations (FWHM) and the transverse velocities of the compact objects. An approximate value of the lens mass is given by

$$M \approx \left(\frac{\text{time} \times V_e}{R_E} \right)^2. \quad (1)$$

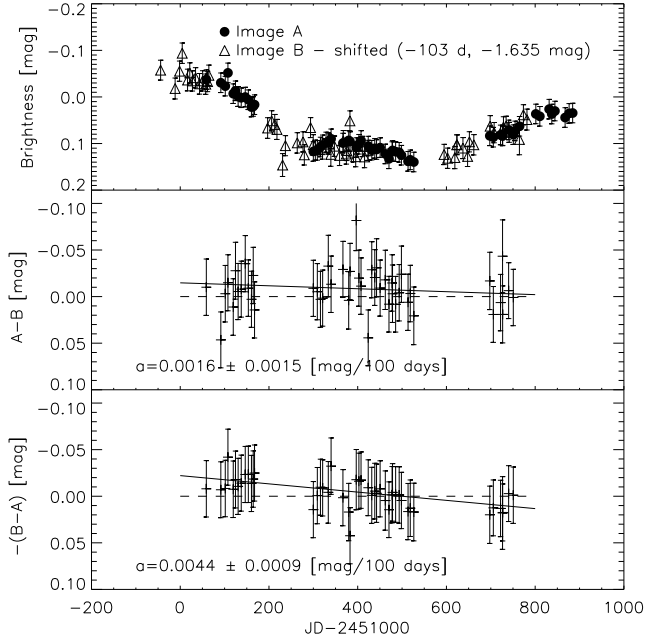


Fig. 3. V-band light curves of HE 2149–2745 and the shifted light curve differences. The middle and bottom panels include linear fits with a being the slope of the linear fit.

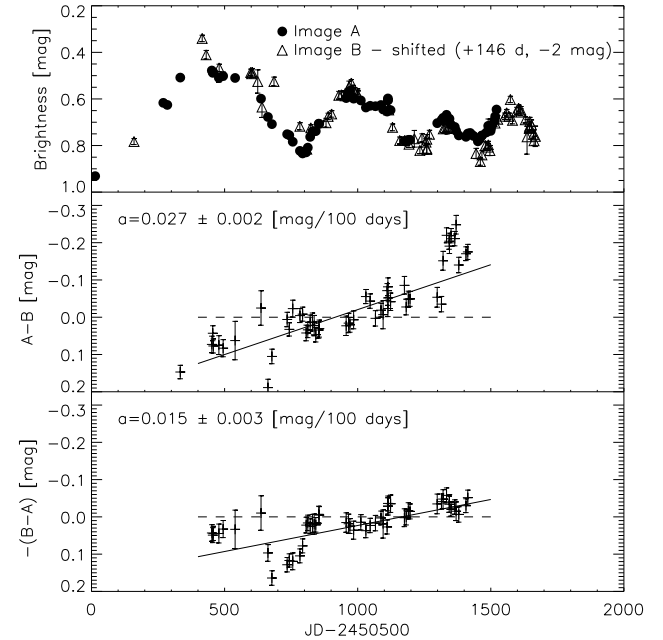


Fig. 4. I-band light curves of RX J0911+055 and the shifted light curve differences. The middle and bottom panels include linear fits with a being the slope of the linear fit.

Here V_e is an effective source velocity, defined as the change in time of the source position measured by the observer, and R_E is the Einstein radius,

$$R_E = \left(\frac{4GM D_{LS} D_S}{c^2 D_L} \right)^{1/2}, \quad (2)$$

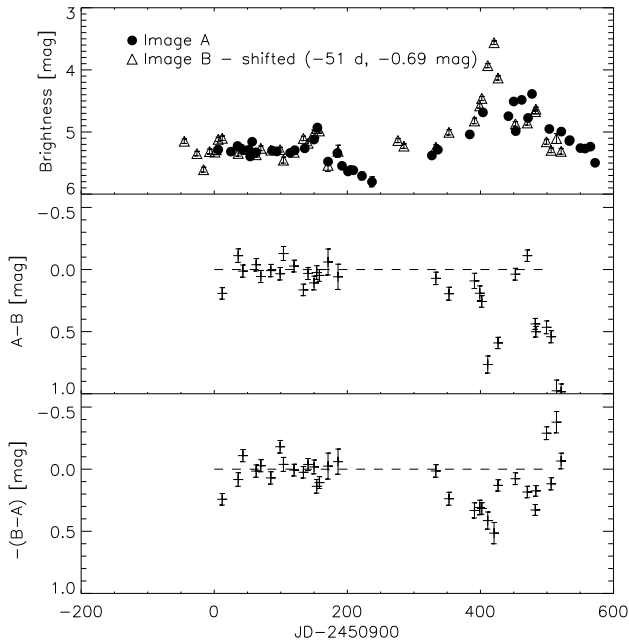


Fig. 5. I-band light curves of B1600+434 and the shifted light curve differences.

where D_{LS} , D_S and D_L are the lens–source, the source–observer and the lens–observer angular diameter distances, respectively.¹

In Table 2 we show the values of possible microlens masses and the corresponding transverse velocities are given by equations (1) and (2). In these calculations we assume that the microlensing is caused by a single compact object. Even with that simplifying assumption, the lens mass can not be determined without knowing the transverse velocity.

There are two possible limits. Due to short duration of the events the microlenses may actually be nanolenses (planets) with masses of order of $10^{-3}M_{\odot}$ for typical transverse velocities of the source of $200\text{--}700\text{ km s}^{-1}$. Similar results were obtained for QSO 0957+561 (Pelt et al. 1998). Conversely, fast microlensing variability can be caused by a solar mass object magnifying small continuum parts of the quasar with relativistic velocities (hot spots) (Schechter et al. 2003) or smooth accretion disk occulted by optically-thick, fast moving clouds (Wyithe & Loeb 2002). Applying this to the two quasars, for microlens mass $1M_{\odot}$, we obtain source (hot spot, cloud) transverse velocities of $0.08c$ for SBS 1520+530 and $0.23c$ for FBQ 0951+2635.

Because of the mass-velocity degeneracy none of these possibilities can be eliminated from a simple analysis. Moreover, we stress that mass determination using equation (1) is only possible for single isolated microlensing events and when the transverse velocity is known. More detailed analyses (Lewis et al. 1993; Wyithe & Turner 2001) assume that the quasar light is affected by numerous compact objects in the

Table 2. Mass-speed relation for SBS 1520+530 and FBQ 0951+2635

Mass [M_{\odot}]	SBS1520+530 Velocity [km/s]	FBQ 0951+2635 Velocity [km/s]
1.0	2.44×10^4	6.87×10^4
0.001	771	2171
0.0001	244	687

foreground galaxy, creating a complex network of caustic lines, and not by a single object (Paczynski 1986).

We conclude that, of the systems we have studied, those with detected flux variability due to microlensing are also reported to have intensity anomalies of spectra continuum and emission line differences. For these systems we have found small linear trends of $\sim 0.005\text{--}0.010\text{ mag}/100\text{ days}$ and bumps with amplitude of $\sim 0.05\text{ mag}$ and durations of $\sim 100\text{ days}$. Interestingly, the systems for which no microlensing variability was detected have no convincing detected microlensing from other methods, although there may be indications in e.g. HE 2149–2745 (Burud et al. 2002a). However, smaller microlensing signals ($\sim 0.005\text{ mag}/100\text{ days}$) in these systems would have been undetectable in our observations.

Acknowledgments. We thank Joachim Wambsganss, Rolf Stabell, Cecile Faure and Jaan Pelt for valuable comments. The Dark Cosmology Centre is funded by the DNRF. This work was carried out within the framework of the EC FP6 Marie Curie Research Training Network ‘‘Astrophysics Network for Galaxy LEnsing Studies (ANGLES)’’. DP acknowledges receipt of a research studentship at the Nordic Optical Telescope. The data used are based on observations made with the Nordic Optical Telescope, operated on the island of La Palma jointly by Denmark, Finland, Iceland, Norway, and Sweden, in the Spanish Observatorio del Roque de los Muchachos of the Instituto de Astrofísica de Canarias.

References

- Burud, I., Hjorth, J., Jaunsen, A. O., et al. 2000, *ApJ*, 544, 117
 Burud, I., Courbin, F., Magain, P., et al. 2002, *A&A*, 383, 71
 Burud, I., Hjorth, J., Courbin, F., et al. 2002, *A&A*, 391, 481
 Chang, K., & Refsdal, S. 1979, *Nature*, 282, 561
 Faure, C., Courbin, F., Kneib, J. P., et al. 2002, *A&A*, 386, 69
 Gaynullina, E. R., Schmidt, R. W., Akhunov, T. et al. 2005, *A&A*, 440, 53
 Hjorth, J., Burud, I., Jaunsen, A. O., et al. 2002, *ApJ*, 572, L11
 Irwin, M. J., Webster, R. L., Hewett, P. C., et al. 1989, *AJ*, 98, 1989
 Jakobsson, P., Hjorth, J., Burud, I., et al. 2005, *A&A*, 431, 103
 Kochanek, C. S. 2004, *ApJ*, 605, 58
 Lewis, G. F., Miralda-Escudé, J., Richardson, D. C., et al. 1993, *MNRAS*, 261, 647
 Paczynski, B. 1986, *ApJ*, 301, 503
 Pelt, J., Schild, R., Refsdal, S., et al. 1998, *A&A*, 336, 829
 Schechter, P. L., Gregg, M. D., Becker, R. H., et al. 1998, *AJ*, 115, 1371
 Schechter, P. L., Udalski, A., Szymański, M., et al. 2003, *ApJ*, 584, 657

¹ We assume a flat universe with $\Omega_m = 0.3$, $\Omega_{\Lambda} = 0.7$ and Hubble constant $H_0 = 70\text{ km s}^{-1}\text{ Mpc}^{-1}$

Schild, R. E. 1990, *AJ*, 100, 1771

Schild, R. E. 1996, *ApJ*, 464, 125

Wyithe, J. S. B., & Turner, E. L. 2001, *MNRAS*, 320, 21

Wyithe, J. S. B., & Loeb, A. 2002, *ApJ*, 577, 615

Table.3. Photometry of two images of FBQ 0951+2635 quasar and two reference stars.

$imag_A$	$imag_B$	$ErrRmag_A$	$ErrImag_B$	$Rmag_{ref1}$	$ErrRmag_{ref1}$	$Rmag_{ref2}$	$ErrRmag_{ref2}$	JD
16.992709	18.034618	0.0122744	0.0126427	19.120347	0.013807705	19.482423	0.014300140	2451176.75
16.949270	17.978877	0.0116044	0.0119707	19.113149	0.013831616	19.492741	0.015953711	2451243.56
16.920836	17.940096	0.0078402	0.0085687	19.130056	0.013900347	19.478551	0.016928954	2451284.35
16.921943	17.921308	0.0106942	0.0111525	19.124617	0.013865446	19.488171	0.016369753	2451293.41
16.903616	17.904475	0.0117503	0.0122057	19.124680	0.013849218	19.524657	0.015659789	2451312.44
16.862798	17.944382	0.0104246	0.0109116	19.134758	0.013842289	19.476014	0.015616346	2451457.71
16.867615	17.936585	0.0103437	0.0108806	19.094160	0.014071862	19.418735	0.022082521	2451485.68
16.880539	17.931990	0.0039793	0.0051447	19.106263	0.013856345	19.421328	0.015121674	2451538.77
16.865312	17.907113	0.0123886	0.0127311	19.147895	0.013857504	19.470908	0.016453767	2451547.63
16.855441	17.873516	0.0125382	0.0127244	19.105739	0.013940485	19.501384	0.022208684	2451587.46
16.841846	17.895178	0.0129032	0.0130755	19.119795	0.013814855	19.504479	0.015086975	2451610.56
16.844951	17.885690	0.0080746	0.0085439	19.124043	0.013794309	19.468493	0.014835601	2451623.40
16.861660	17.898676	0.0105123	0.0110129	19.104203	0.013865219	19.456326	0.015949634	2451675.41
16.863279	17.899549	0.0103627	0.0106677	19.124836	0.013788088	19.499720	0.014183901	2451682.38
16.880199	17.916674	0.0120163	0.0123721	19.112471	0.013880340	19.519183	0.018577257	2451696.40
16.871481	17.934753	0.0095932	0.0101394	19.133569	0.013859803	19.490971	0.016356478	2451723.39
16.891041	17.986269	0.0109143	0.0114012	19.119965	0.013834873	19.481175	0.015792936	2451821.75
16.896003	17.955737	0.0111720	0.0113642	19.136559	0.013828723	19.480894	0.015218081	2451834.73
16.879795	17.970869	0.0126409	0.0128128	19.096878	0.013967582	19.436984	0.017929207	2451845.73
16.894209	17.943196	0.0042684	0.0056762	19.140959	0.013870139	19.497979	0.015667505	2451851.76
16.872078	17.953676	0.0085913	0.0091732	19.126812	0.013863490	19.521216	0.016408040	2451865.73
16.882127	17.955942	0.0125129	0.0128133	19.153717	0.013810298	19.505930	0.015129165	2451870.76
16.888764	17.929586	0.0122424	0.0126007	19.131944	0.013797467	19.487918	0.014854928	2451880.74
16.893100	17.945269	0.0123475	0.0126993	19.114313	0.013926707	19.511076	0.020537456	2451907.76
16.887662	17.972687	0.0122124	0.0123627	19.105902	0.013820950	19.475602	0.014776934	2451914.55
16.896969	17.969818	0.0095270	0.0100416	19.146569	0.013860617	19.493764	0.016385478	2451923.66
16.897377	17.958831	0.0120538	0.0124478	19.135314	0.013811676	19.493437	0.014292094	2451928.57
16.898735	17.955738	0.0126376	0.0129884	19.124129	0.013826723	19.503457	0.014864473	2451959.52
16.884034	17.969461	0.0042291	0.0055371	19.120140	0.013817373	19.520684	0.014550879	2451967.62
16.884285	17.954437	0.0126648	0.0130048	19.144934	0.013794118	19.534463	0.015241120	2451983.47
16.889696	17.956140	0.0130337	0.0131508	19.119829	0.013884220	19.533765	0.017750150	2451999.36
16.886299	17.960918	0.0134442	0.0135783	19.121428	0.013821902	19.496912	0.015105136	2452000.35
16.895846	17.932691	0.0103642	0.0106085	19.094316	0.013906281	19.449698	0.016586867	2452007.48
16.885167	17.948287	0.0129423	0.0130618	19.130773	0.013812789	19.525274	0.014868060	2452014.38
16.898816	17.953915	0.0086892	0.0091713	19.148099	0.013932938	19.527538	0.021234268	2452016.40
16.917229	17.951211	0.0134910	0.0136049	19.147977	0.013812686	19.508021	0.014486790	2452022.39
16.923007	17.965599	0.0129227	0.0130598	19.148200	0.013777790	19.500059	0.014440096	2452026.42
16.906482	17.981935	0.0111480	0.0113552	19.144386	0.013771457	19.489314	0.013947707	2452030.44
16.895825	17.965255	0.0121185	0.0123055	19.085406	0.013906838	19.462510	0.017683878	2452008.36
16.909523	17.965818	0.0133956	0.0134637	19.107931	0.013836224	19.481380	0.016996284	2452013.42
16.922141	17.975225	0.0103913	0.0106341	19.135155	0.013781629	19.496244	0.014553395	2452033.42
16.929039	17.991203	0.0129533	0.0130885	19.127224	0.013838793	19.486634	0.014117430	2452047.40
16.927728	18.001496	0.0130892	0.0132157	19.128467	0.013777552	19.514531	0.014502249	2452051.39
16.929106	18.025580	0.0131267	0.0132529	19.134794	0.013780329	19.509152	0.014461936	2452055.40
16.936453	18.009050	0.0106027	0.0108315	19.159283	0.013819508	19.512907	0.016321199	2452058.38
16.943759	17.959676	0.0081699	0.0086049	19.156133	0.013809766	19.522428	0.015438366	2452059.38
16.933074	18.014459	0.0068614	0.0073612	19.141548	0.013765144	19.505601	0.014014124	2452060.38
16.937465	18.054031	0.0121674	0.0123452	19.141910	0.013834839	19.511048	0.015714603	2452077.39
16.944463	18.026573	0.0115327	0.0117283	19.108928	0.013834722	19.455369	0.015313457	2452081.38
16.851988	17.883746	0.0062832	0.0084698	19.126692	0.013782970	19.501844	0.014435887	2451466.77
16.870338	17.913338	0.0105393	0.0111023	19.126316	0.013781707	19.512694	0.014083847	2451471.72
16.844608	17.863082	0.0067235	0.0072235	19.134932	0.013783441	19.511825	0.014415147	2451596.57
16.866450	17.906396	0.0045824	0.0061145	19.133440	0.013831234	19.486610	0.016333501	2451703.40
16.866219	17.944543	0.0109743	0.0112793	19.101035	0.013877617	19.468187	0.017442770	2451861.73
16.867510	17.968184	0.0076510	0.0094711	19.136351	0.013891461	19.503001	0.017352248	2451945.68
16.880295	17.929751	0.0040531	0.0054936	19.099264	0.014002759	19.455817	0.017569236	2452003.37
16.907873	17.972477	0.0111268	0.0114910	19.137579	0.013797823	19.509583	0.014943108	2452037.42
16.921842	17.998561	0.0044078	0.0071272	19.147866	0.013811678	19.487119	0.015711978	2452071.38

Table.4. Photometry of two images of B1600+434 quasar.

<i>imag_A</i>	<i>ErrImag_A</i>	<i>imag_B</i>	<i>ErrImag_B</i>	JD
5.2819	0.0296	5.8385	0.0356	2450906.00
5.3158	0.0315	6.0376	0.0362	2450925.00
5.2249	0.0324	6.2962	0.0395	2450935.00
5.2928	0.0288	6.0041	0.0402	2450944.00
5.2868	0.0295	6.0137	0.0387	2450952.00
5.3941	0.0295	5.9756	0.0360	2450954.00
5.1570	0.0315	5.8081	0.0356	2450957.00
5.3272	0.0285	5.7904	0.0358	2450963.00
5.2983	0.0283	6.0343	0.0446	2450987.00
5.3121	0.0298	5.9627	0.0367	2450994.00
5.3363	0.0287	6.0556	0.0404	2451014.00
5.2926	0.0291	5.9526	0.0385	2451021.00
5.2632	0.0289	5.9821	0.0398	2451036.00
5.1212	0.0305	5.9744	0.0390	2451050.00
4.9277	0.0301	6.1430	0.0486	2451055.00
5.4757	0.0284	6.0166	0.0378	2451071.00
5.3390	0.0283	5.7932	0.0353	2451085.00
5.5449	0.0292	5.8710	0.0388	2451092.00
5.6352	0.0420	5.7032	0.0471	2451101.00
5.6096	0.0461	5.6322	0.0468	2451105.00
5.6159	0.0329	5.6729	0.0363	2451109.00
5.7076	0.0604	6.2264	0.1002	2451122.00
5.8021	0.0805	5.9997	0.0974	2451137.00
5.3782	0.0297	5.8271	0.0333	2451227.00
5.2853	0.0291	5.9171	0.0364	2451236.00
5.0390	0.0297	5.9352	0.0413	2451284.00
4.6846	0.0300	5.6948	0.0430	2451303.75
4.7455	0.0283	5.5117	0.0445	2451342.00
4.5086	0.0322	5.2692	0.0361	2451350.00
4.9867	0.0321	5.1490	0.0328	2451353.00
4.4828	0.0327	4.6215	0.0332	2451362.00
4.7733	0.0422	4.2523	0.0292	2451371.50
4.3872	0.0333	4.8200	0.0344	2451377.50
4.9513	0.0290	5.5594	0.0373	2451403.50
4.9932	0.0297	5.5444	0.0353	2451421.50
5.1450	0.0300	5.3622	0.0319	2451433.50
5.1311	0.0303	5.3218	0.0318	2451434.25
5.2592	0.0283	5.8469	0.0400	2451450.25
5.2670	0.0315	5.9853	0.0365	2451457.25
5.2361	0.0446	5.7947	0.0795	2451465.25
5.4954	0.0295	6.0011	0.0465	2451472.25

Table.5.Photometry of two images of HE 2149-2745 quasar in i-band.

<i>imag_A</i>	<i>ErrImag_A</i>	<i>imag_B</i>	<i>ErrImag_B</i>	JD
1.58210003	0.0378655307	3.06310010	0.0389079675	2451091.5
1.57809997	0.0378287919	3.07520008	0.0383489877	2451058.7
1.56980002	0.0378377251	3.04200006	0.0384890176	2451100.5
1.64760005	0.0378425010	3.10999990	0.0385378115	2451107.5
1.53980005	0.0378421955	3.01279998	0.0385516994	2451114.5
1.60200000	0.0378793776	3.07660007	0.0391337611	2451119.5
1.60819995	0.0378611907	3.06750011	0.0388117172	2451137.5
1.61109996	0.0378544070	3.05719995	0.0387288556	2451124.5
1.57679999	0.0378506258	3.03020000	0.0386729501	2451130.5
1.60739994	0.0378769375	3.08220005	0.0391000696	2451146.5
1.62779999	0.0378769971	3.09910011	0.0390986577	2451160.5
1.62199998	0.0378788561	3.06690001	0.0390518941	2451164.5
1.62600005	0.0378556550	3.04169989	0.0387061089	2451167.5
1.61249995	0.0378501825	3.06040001	0.0386340357	2451153.5
1.69700003	0.0378291346	3.13479996	0.0383005626	2451315.0
1.69659996	0.0379458442	3.13969994	0.0400222652	2451333.7
1.66649997	0.0378436223	3.12859988	0.0385885425	2451349.0
1.70169997	0.0378417931	3.14669991	0.0384832397	2451309.0
1.68959999	0.0378342941	3.13730001	0.0383743569	2451321.0
1.68879998	0.0378567949	3.14389992	0.0387759842	2451367.2
1.68270004	0.0378336124	3.12899995	0.0383646935	2451424.5
1.70990002	0.0378260836	3.15849996	0.0382536501	2451431.7
1.71210003	0.0378338359	3.17630005	0.0383979045	2451379.7
1.66729999	0.0378314964	3.16689992	0.0383910239	2451382.7
1.69579995	0.0378432684	3.18959999	0.0385701284	2451438.5
1.73540003	0.0378137380	3.26299996	0.0392147452	2451844.5
1.69760001	0.0378320850	3.15790009	0.0383670107	2451450.5
1.67579997	0.0378207192	3.22160006	0.0382636935	2451396.7
1.70350003	0.0378232971	3.17950010	0.0382370576	2451402.5
1.69690001	0.0378274396	3.18779993	0.0383255184	2451408.5
1.68819997	0.0378242321	3.20910010	0.0382717140	2451791.7
1.72570002	0.0378414802	3.19670010	0.0385198407	2451462.5
1.68330002	0.0379273593	3.15470004	0.0398344211	2451471.5
1.69990003	0.0378282033	3.21900010	0.0383800194	2451479.5
1.71200001	0.0378198288	3.20230007	0.0381722786	2451484.5
1.73169994	0.0378440991	3.21190000	0.0385658108	2451519.5
1.71099997	0.0378429405	3.23639989	0.0386381000	2451823.7
1.67690003	0.0378333218	3.19930005	0.0384436920	2451831.5
1.68209997	0.0378317647	3.18689993	0.0384052061	2451750.7
1.70089996	0.0379198268	3.22169995	0.0398468710	2451754.7

Table.6. Photometry of two images of quasar HE 2149-2745 in V-band.

$imag_A$	$ErrImag_A$	$imag_B$	$ErrImag_B$	JD
- 0.0304	0.0209	1.6168	0.0224	2451091.50
- 0.0372	0.0210	1.5774	0.0213	2451058.75
- 0.0231	0.0210	1.5796	0.0217	2451101.50
- 0.0070	0.0210	1.5987	0.0232	2451119.50
- 0.0131	0.0210	1.5835	0.0216	2451124.50
- 0.0006	0.0210	1.6006	0.0217	2451130.50
0.0017	0.0210	1.5937	0.0216	2451137.50
- 0.0516	0.0210	1.5411	0.0219	2451107.50
0.1087	0.0210	1.7007	0.0214	2451396.75
0.0001	0.0210	1.6068	0.0221	2451146.50
0.0060	0.0210	1.6004	0.0217	2451153.50
0.0218	0.0210	1.6075	0.0217	2451160.50
0.0205	0.0210	1.6017	0.0218	2451164.50
0.0165	0.0210	1.5885	0.0218	2451167.50
0.1169	0.0210	1.7016	0.0221	2451300.00
0.1146	0.0210	1.6862	0.0215	2451309.00
0.1075	0.0210	1.6941	0.0215	2451316.00
0.1027	0.0210	1.7046	0.0215	2451321.00
0.0983	0.0210	1.7812	0.0245	2451333.75
0.0899	0.0210	1.7395	0.0215	2451340.00
0.0989	0.0210	1.7336	0.0218	2451366.75
0.0932	0.0210	1.7315	0.0216	2451379.75
0.0957	0.0210	1.7592	0.0217	2451382.75
0.1015	0.0210	1.7374	0.0215	2451402.75
0.1054	0.0210	1.7468	0.0216	2451423.75
0.1102	0.0210	1.7361	0.0216	2451438.50
0.1142	0.0210	1.7321	0.0215	2451431.75
0.0935	0.0210	1.7491	0.0215	2451407.50
0.1128	0.0210	1.7582	0.0255	2451442.50
0.1088	0.0210	1.7407	0.0218	2451450.50
0.1222	0.0210	1.7605	0.0216	2451462.25
0.1327	0.0210	1.7295	0.0224	2451470.50
0.1172	0.0210	1.7575	0.0216	2451477.50
0.1147	0.0210	1.7500	0.0215	2451478.50
0.1176	0.0210	1.6863	0.0213	2451485.50
0.1187	0.0210	1.7534	0.0212	2451493.50
0.1251	0.0210	1.7632	0.0215	2451498.50
0.1382	0.0210	1.7414	0.0218	2451513.50
0.1350	0.0210	1.7638	0.0230	2451518.50
0.1396	0.0210	1.7496	0.0215	2451526.50
0.0815	0.0210	1.7651	0.0238	2451722.00
0.0830	0.0210	1.7375	0.0212	2451726.75
0.0864	0.0210	1.7666	0.0217	2451705.75
0.0707	0.0210	1.7447	0.0225	2451740.25
0.0838	0.0210	1.7375	0.0212	2451726.50
0.0834	0.0210	1.7584	0.0217	2451697.75
0.0810	0.0210	1.7625	0.0217	2451750.75
0.0728	0.0210	1.7313	0.0216	2451754.75
0.0630	0.0210	1.7376	0.0218	2451764.75
0.0364	0.0210	1.6978	0.0227	2451801.50
0.0416	0.0210	1.7115	0.0217	2451810.50
0.0262	0.0210	1.6997	0.0222	2451831.50
0.0366	0.0210	1.6977	0.0213	2451837.50
0.0302	0.0210	1.7109	0.0213	2451844.50
0.0441	0.0210	1.7261	0.0328	2451867.50
0.0344	0.0210	1.6835	0.0224	2451884.50
0.0353	0.0210	1.6734	0.0217	2451876.50

Table.7. Photometry of two images of quasar RX J0911+0551.

<i>imag_A</i>	<i>ErrImag_A</i>	<i>imag_B</i>	<i>ErrImag_B</i>	JD
17.4314	0.012097	19.2829	0.012846	2450513.75
17.1167	0.012261	18.8402	0.013740	2450769.75
17.1257	0.013128	18.9104	0.018604	2450784.75
17.0083	0.011679	18.9664	0.015633	2450833.50
16.9780	0.012216	18.9863	0.014306	2450952.00
16.9878	0.012588	18.9918	0.017682	2450955.50
16.9855	0.012432	18.9854	0.016262	2450957.50
17.0099	0.018110	19.0251	0.049982	2450978.50
17.0016	0.016199	19.1349	0.044582	2450994.50
17.0099	0.012700	19.0251	0.018789	2451039.50
17.0989	0.012273	19.2174	0.015305	2451136.75
17.1774	0.012200	19.3156	0.014460	2451162.75
17.2081	0.012094	19.2239	0.012973	2451177.75
17.2514	0.012870	19.2023	0.019072	2451235.00
17.2558	0.012188	19.1749	0.013675	2451243.00
17.2838	0.012242	19.1644	0.013936	2451256.00
17.3230	0.012786	19.0844	0.016953	2451283.00
17.3340	0.012643	19.0819	0.016079	2451293.00
17.3293	0.012319	19.0868	0.014112	2451306.50
17.3090	0.013496	19.0787	0.020718	2451312.50
17.2628	0.014121	19.0474	0.024044	2451321.50
17.2391	0.012372	19.0314	0.014646	2451330.00
17.2386	0.012744	19.0592	0.017307	2451336.50
17.2382	0.012927	19.0693	0.018480	2451342.50
17.2060	0.013608	19.0799	0.022970	2451353.50
17.2071	0.013444	19.0877	0.022186	2451355.50
17.0963	0.012342	19.1293	0.015669	2451456.75
17.0719	0.012927	19.1268	0.020853	2451465.75
17.0660	0.012393	19.1474	0.016441	2451470.75
17.0987	0.012193	19.2220	0.014468	2451484.75
17.1064	0.012217	19.2785	0.015011	2451511.75
17.1368	0.012188	19.2781	0.014460	2451530.75
17.1294	0.012145	19.2944	0.013966	2451546.75
17.1312	0.014747	19.2710	0.035811	2451566.75
17.1260	0.012167	19.3209	0.014371	2451587.50
17.1453	0.012479	19.2673	0.017630	2451595.50
17.1542	0.012282	19.2853	0.015319	2451610.50
17.1049	0.012669	19.3130	0.020335	2451613.50
17.0979	0.012658	19.2729	0.019833	2451613.50
17.1058	0.012671	19.3169	0.020383	2451613.50
17.1481	0.012445	19.2519	0.017215	2451623.50
17.2804	0.012584	19.2286	0.017100	2451675.50
17.2842	0.012405	19.2229	0.015676	2451682.25
17.2756	0.013434	19.2272	0.023092	2451690.25
17.2754	0.012512	19.2225	0.016512	2451696.50
17.2040	0.012910	19.3341	0.021965	2451798.75
17.1908	0.012287	19.3688	0.015887	2451814.75
17.1812	0.012463	19.3403	0.017784	2451820.75
17.1682	0.012275	19.2998	0.015553	2451833.75
17.1901	0.012176	19.3068	0.014179	2451843.75
17.1850	0.012226	19.2968	0.014778	2451844.75
17.2105	0.012952	19.3215	0.021781	2451850.75

continued on next page.

continued from previous page.				
<i>imag_A</i>	<i>ErrImag_A</i>	<i>imag_B</i>	<i>ErrImag_B</i>	JD
17.2203	0.012489	19.1839	0.016541	2451864.75
17.2371	0.012213	19.2037	0.013989	2451869.75
17.2566	0.012470	19.1875	0.016057	2451879.75
17.2626	0.012195	19.1742	0.013649	2451906.75
17.2484	0.012238	19.1593	0.014067	2451913.50
17.2460	0.012263	19.1749	0.014233	2451922.50
17.2528	0.012202	19.1022	0.013505	2451927.50
17.2591	0.012341	19.1918	0.014997	2451935.50
17.2820	0.012366	19.1509	0.014891	2451951.50
17.2727	0.012207	19.1396	0.013631	2451958.50
17.2574	0.012254	19.1466	0.014101	2451966.50
17.2570	0.012309	19.1568	0.014555	2451966.50
17.2437	0.012180	19.1896	0.013604	2451983.50
17.2155	0.029405	19.2627	0.074262	2451990.25
17.2330	0.012209	19.2268	0.014023	2451998.50
17.2372	0.012308	19.2229	0.014987	2451999.25
17.2247	0.012686	19.2174	0.017995	2451999.75
17.2250	0.012686	19.1970	0.017995	2452000.25
17.2093	0.013035	19.2109	0.020981	2452006.50
17.1904	0.012433	19.2521	0.016423	2452014.50
17.1750	0.012724	19.2797	0.019634	2452016.50
17.1454	0.006381	19.2605	0.043823	2452021.50

Table.8. Photometry of two images of SBS 1520+530 quasar.

<i>imag_A</i>	<i>ErrImag_A</i>	<i>imag_B</i>	<i>ErrImag_B</i>	JD
1.2548	0.01430	1.8684	0.02422	2451226.75
1.1809	0.00911	1.8650	0.01154	2451235.75
1.2221	0.00876	1.8486	0.00967	2451243.75
1.2245	0.00875	1.8931	0.00970	2451255.75
1.1905	0.00869	1.8935	0.00966	2451264.75
1.2312	0.00869	1.9357	0.00957	2451284.50
1.2257	0.00873	1.9430	0.00981	2451306.50
1.2154	0.00879	1.9373	0.01016	2451311.50
1.1879	0.00871	1.9115	0.00978	2451319.50
1.1747	0.00867	1.9314	0.00960	2451336.50
1.1725	0.00873	1.9221	0.00997	2451342.50
1.1629	0.00871	1.9154	0.00978	2451354.50
1.1426	0.00859	1.9055	0.00911	2451362.50
1.1448	0.00891	1.9151	0.01090	2451371.50
1.1341	0.00860	1.9162	0.00922	2451377.50
1.1426	0.00867	1.9214	0.00960	2451386.50
1.1525	0.00877	1.9316	0.01021	2451403.50
1.1515	0.00864	1.9627	0.00953	2451420.25
1.1293	0.00857	1.9227	0.00900	2451433.25
1.1310	0.00856	1.9197	0.00898	2451434.25
1.1341	0.00898	1.8800	0.00962	2451443.25
1.1406	0.00860	1.8994	0.00916	2451450.25
1.1449	0.00877	1.8658	0.00999	2451457.25
1.1433	0.00892	1.8503	0.01074	2451465.25
1.0952	0.00871	1.8334	0.00966	2451530.75
1.1086	0.00867	1.8229	0.00944	2451566.75
1.1139	0.00870	1.8227	0.00963	2451586.75
1.0913	0.00868	1.8227	0.00959	2451609.50
1.1137	0.00890	1.8154	0.01048	2451613.75
1.1094	0.00869	1.7793	0.00961	2451674.50
1.1107	0.00869	1.7898	0.00947	2451683.50
1.1174	0.00883	1.7758	0.01016	2451689.50
1.1111	0.00867	1.8072	0.00953	2451695.50
1.0908	0.00879	1.7812	0.01000	2451703.50
1.0908	0.01052	1.8043	0.01639	2451715.50
1.0869	0.00866	1.7966	0.00955	2451723.50
1.0907	0.00866	1.8130	0.00961	2451730.50
1.1080	0.00861	1.8403	0.00918	2451751.50
1.0948	0.00871	1.8317	0.00974	2451765.50
1.0880	0.00859	1.8285	0.00913	2451781.50
1.0747	0.00860	1.8415	0.00913	2451793.50
1.0588	0.00857	1.8399	0.00900	2451799.25
1.0616	0.00858	1.8407	0.00902	2451807.50
1.0468	0.00877	1.8561	0.01026	2451815.25
1.0013	0.00864	1.8408	0.00948	2451834.25
0.9944	0.00882	1.8408	0.01070	2451869.75
1.1008	0.00867	1.8286	0.00945	2451907.75
1.1141	0.00857	1.8240	0.00891	2451913.75
1.1446	0.00863	1.8035	0.00911	2451922.75
1.1587	0.00871	1.7976	0.00950	2451927.75
1.1866	0.00865	1.7408	0.00904	2451950.75
1.1964	0.00871	1.7304	0.00934	2451958.75
1.2070	0.00876	1.7117	0.00938	2451966.50
1.2178	0.00899	1.7128	0.00995	2451975.75
1.2139	0.00864	1.7222	0.00896	2451983.75
1.2220	0.00865	1.7232	0.00898	2451984.75
1.2168	0.00901	1.7594	0.01011	2452007.50
1.2446	0.00874	1.7632	0.00932	2452007.75